

Dual-band bandpass tunable microwave photonic filter based on stimulated Brillouin scattering*

LI Jia-qi (李嘉琪)¹, XIAO Yong-chuan (肖永川)², DONG Wei (董玮)^{1**}, and ZHANG Xin-dong (张歆东)¹

1. State Key Laboratory on Integrated Optoelectronics, College of Electronic Science and Engineering, Jilin University, Changchun 130012, China

2. Chongqing Optoelectronics Research Institute, Chongqing 400060, China

(Received 29 April 2016)

©Tianjin University of Technology and Springer-Verlag Berlin Heidelberg 2016

A dual-band bandpass microwave photonic filter (MPF) based on stimulated Brillouin scattering (SBS) is theoretically analyzed and experimentally demonstrated. Two separated tunable laser sources (TLSs) are employed to generate two passbands by implementing phase modulation to amplitude modulation conversion by using SBS induced sideband amplification. The center frequencies of both passbands can be independently tuned ranging from 1 GHz to 19 GHz. High resolution with 3 dB bandwidth less than 30 MHz and large out-of-band rejection about 40 dB under 25 mW optical pump power are achieved.

Document code: A **Article ID:** 1673-1905(2016)04-0276-4

DOI 10.1007/s11801-016-6109-z

For application in wireless communication systems, dual-band bandpass microwave filters have been researched in electrical domain to distinguish different wireless communication standards^[1]. However, most dual-band bandpass microwave filters have poor or even lack of tuning capability, which limits the filters' performance for signal processing^[2]. A promising candidate based on photonic-assisted microwave filtering has been investigated to offer a more powerful solution to process microwave and millimeter wave signals directly in the optical domain, enabling flexible tunability and reconfigurability, broad bandwidth, and strong anti-electromagnetic interference ability^[3,4]. One configuration has been demonstrated to produce two independently tunable passbands using an equivalent phase-shifted Bragg grating fiber by converting phase modulation to amplitude modulation^[5]. The frequency tunable ranges are 5.4 GHz and 7.4 GHz for the first and second passbands, respectively and the corresponding 3 dB bandwidths are 167.3 MHz and 143.3 MHz, respectively.

Recently, stimulated Brillouin scattering (SBS) effect has been used to implement high-resolution and broad-tuning-range microwave photonic filter (MPF) due to its intrinsic narrow band and large flexibility^[6-9]. In this paper, a novel dual-band bandpass MPF based on phase modulation and SBS induced sideband amplification is analyzed and experimentally demonstrated. Two tunable laser sources (TLSs) are provided to generate two irrelative gain spectra that contribute to generation of two passbands via the phase to intensity modulation conver-

sion. This enables independent tuning of the two passbands by simply changing the output frequencies of the two pump lasers. Experimental results demonstrate the frequency tunability in the range from 1 GHz to 19 GHz for both passbands. High resolution with 3 dB bandwidth about 30 MHz and large out-of-band rejection about 40 dB under 25 mW optical pump power are obtained.

The SBS effect in fiber is known as a nonlinear interaction involving two counter-propagating light waves and an acoustic wave. When the phase matching condition is satisfied: $f_{\text{Stokes}} = f_{\text{pump}} - \nu_B$ (ν_B is Brillouin frequency shift), the power will be transferred from pump wave to the Stokes wave, leading to amplification for Stokes wave. The gain of SBS process can be described as follows:

$$g(f) = \frac{g_B I_p}{2} \frac{(\Delta\nu_B / 2)^2}{(f + \nu_B - f_p)^2 + (\Delta\nu_B / 2)^2} + j \frac{g_B I_p}{4} \frac{\Delta\nu_B (f + \nu_B - f_p)}{(f + \nu_B - f_p)^2 + (\Delta\nu_B / 2)^2}, \quad (1)$$

where g_B and $\Delta\nu_B$ represent the line-center gain factor and Brillouin linewidth, respectively, $I_p = P_p / A_{\text{eff}}$ (A_{eff} is the fiber effective area) is the intensity of pump wave, f_p denotes the pump wave frequency, and f is the frequency deviation from the gain center.

Fig.1 shows the block diagram of the proposed dual-band bandpass MPF. The upper path is a simple

* This work has been supported by the Science and Technology Development Plan of Jilin Province (Nos.20150204003GX and 20160519010JH), and the Science and Technology Plan of Changchun (No.14KG019).

** E-mail:dongw@jlu.edu.cn

phase modulation link consisting of TLS1, phase modulator (PM), highly nonlinear fiber (HNLF), etc. Since RF signals after phase modulation cannot be detected directly by square-law detector in optical link, its transfer function gives a stopband response. Hence, the Brillouin induced sideband amplification can be employed to implement phase-to-amplitude modulation conversion, thus generating filter passband. Due to one pump wave forms one gain region, two pumps can enable the generation of two gain regions. In this paper, two irrelative tunable laser sources, TLS2 and TLS3, are provided to produce two gain regions required, which is shown as the lower path in Fig.1. By mapping these two gains, the dual-band bandpass filter response can be obtained. Furthermore, these two passbands can be independently tuned by adjusting the frequencies of TLS2 and TLS3. The spectrum processing is demonstrated in Fig.2, where pump1 and pump2 refer to TLS2 and TLS3, respectively. It is worth noting that the SBS effect will generate a loss spectrum in higher frequency region, causing an undesired passband. Since the Brillouin frequency shift of our HNLF is around 10 GHz, the higher frequency passband can be eliminated by choosing a photodetector (PD) or PM with a bandwidth of 20 GHz.

For small-signal modulation, the output optical field after phase modulation can be expressed as:

$$E(t) = J_0(m) \exp(j2\pi f_c t) + J_1(m) \exp\left\{j\left[2\pi(f_c + f_m)t + \frac{\pi}{2}\right]\right\} - J_1(m) \exp\left\{j\left[2\pi(f_c - f_m)t - \frac{\pi}{2}\right]\right\}, \quad (2)$$

where f_c is carrier frequency and f_m is modulation frequency, $J_n(\bullet)$ represents the n th-order Bessel function of the first kind with $n=0, \pm 1$, and m is the modulation index associated to modulator frequency response. When introducing SBS effect, the transmission optical field can be written as:

$$E(t) = J_0(m) \exp(j2\pi f_c t) - J_1(m) \exp\left\{j\left[2\pi(f_c - f_m)t - \frac{\pi}{2}\right]\right\} + J_1(m) \exp\left\{j\left[2\pi(f_c + f_m)t + \frac{\pi}{2}\right] + G_1(f_m) + G_2(f_m)\right\}, \quad (3)$$

where

$$G_1(f_m) = g\left[(f_c + f_m) - (f_{p1} - \nu_B)\right],$$

$$G_2(f_m) = g\left[(f_c + f_m) - (f_{p2} - \nu_B)\right]. \quad (4)$$

Omitting the direct current and the small second harmonic components, the output electronic field after de-

tection can be given as:

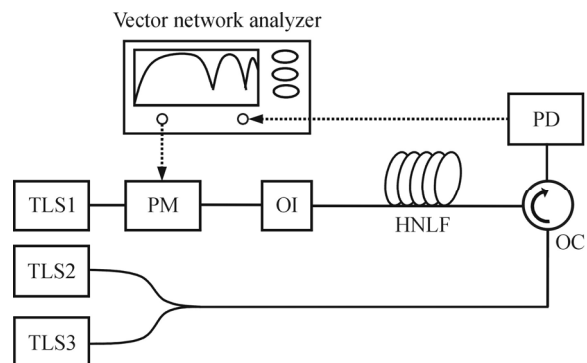
$$E_{rf}(t) = \Re\left\langle |E(t)|^2 \right\rangle \propto \exp\left\{\text{Re}\left[G_1(f_m) + G_2(f_m)\right]\right\} \cos\left\{2\pi f_m t + \text{Im}\left[G_1(f_m) + G_2(f_m)\right] + \frac{\pi}{2}\right\} - \cos\left(2\pi f_m t + \frac{\pi}{2}\right), \quad (5)$$

where \Re means the responsivity of PD depending on the modulation frequency and $\langle \rangle$ represents the ensemble average of the signal.

Therefore, the normalized transfer function of the structure can be written as:

$$|H(f_m)|^2 = \exp\left\{2\text{Re}\left[G_1(f_m) + G_2(f_m)\right]\right\} + 1 - 2\exp\left\{\text{Re}\left[G_1(f_m) + G_2(f_m)\right]\right\} \cos\left\{\text{Im}\left[G_1(f_m) + G_2(f_m)\right]\right\}. \quad (6)$$

We have implemented the dual-band bandpass MPF based on the configuration in Fig.1. The output frequency of TLS1 as carrier is set to be 193.41 THz (~1 550 nm). Subsequently, it is modulated with PM driven by vector network analyzer (VNA)-launched frequency-swept RF signal. Then the phase-modulated optical signal is directed to HNLF via optical isolator (OI) for further processing. On the other hand, TLS2 and TLS3 regarded as pump1 and pump2 respectively are coupled through optical circulator (OC) into the HNLF from the other end. Adjusting the frequencies of TLS2 and TLS3 to be larger than that of TLS1, the upper sidebands are amplified as designed in Fig.2. Finally, the transfer function is measured by VNA after detection. Fig.3 shows an example of the frequency response of the dual-band bandpass MPF. The optical power of the pump waves is around 10 mW. The passband1 is generated by mapping the gain spectrum induced by pump1, while the passband2 is generated by mapping the gain spectrum of pump2.



TLS: tunable laser source; PC: polarization controller; PM: phase modulator; HNLF: highly nonlinear fiber; OI: optical isolator; OC: optical circulator; PD: photodetector

Fig.1 Experimental setup of the proposed dual-band bandpass MPF

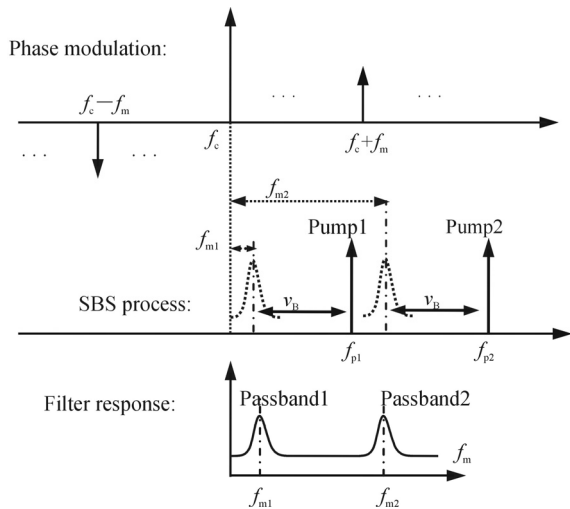


Fig.2 Spectrum processing for the generation of dual-band passband response

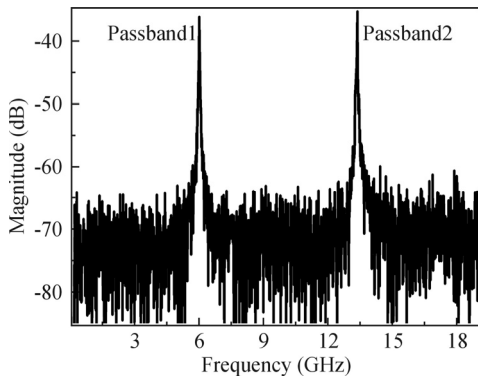


Fig.3 Frequency response of the dual-band bandpass filter

Firstly, we investigate the filter performance of the proposed structure. Since the passbands are independently generated by two identical pump lasers, we can use one of the pumps to characterize the filter performance. Here TLS3 is switched off and then the frequency space is changed between TLS1 and TLS2 to generate a single passband as shown in Fig.4(a). The filter response over the frequency span of 19 GHz is demonstrated. It can be seen that the peak of filter passband increases with the pump power. This also leads to an approximately linear improvement for out-of-band rejection as illustrated in Fig.4(b). The maximum attainable value is 41 dB when the pump power reaches 25 mW which is the highest value for our available laser source. Fig.5(a) is the detailed view of filter passband. After Lorentz fitting, filter bandwidth as a function of pump power is plotted in Fig.5(b).

Then we switch on TLS3 and change the output frequencies of both pumps to demonstrate the independently tuning of the two passbands. On the one hand, we fix the passband1 at frequency around 1 GHz and tune passband2 as shown in Fig.6(a). And on the other hand, the passband2 is fixed around 19 GHz and the passband1 is

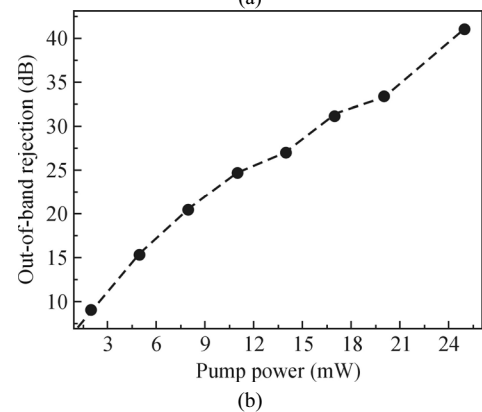
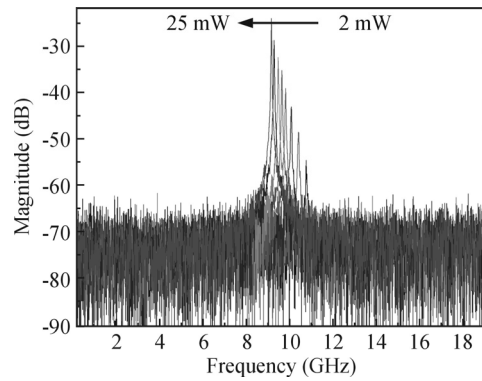


Fig.4 (a) Frequency responses for different pump power under single pump wave condition; (b) Out-of-band rejection as a function of pump power

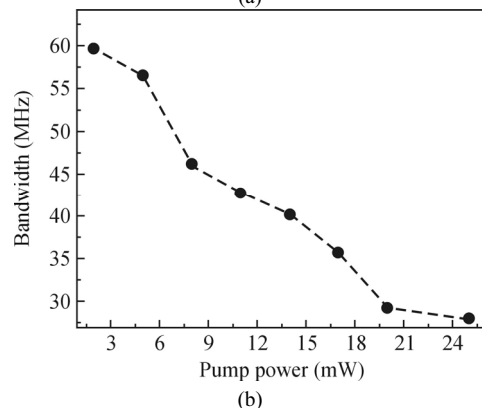
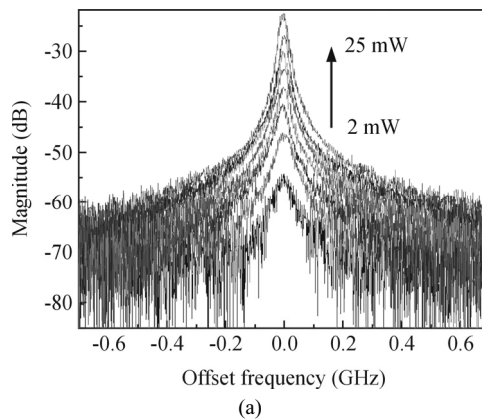


Fig.5 (a) Zoom-in view of the filter passband; (b) Filter 3 dB bandwidth variation for different pump power

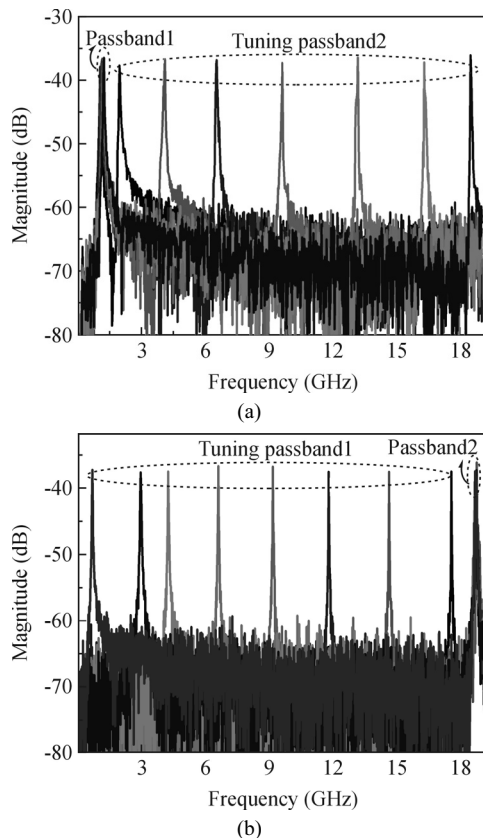


Fig.6 (a) Frequency response when passband1 is fixed and passband2 is tuned; (b) Frequency response when passband2 is fixed and passband1 is tuned

tuned as shown in Fig.6(b). Consequently, arbitrary tuning from 1 GHz to 19 GHz is experimentally verified for both passbands. Notice that the product of modulation efficiency and detector responsivity decreases as the modulation frequency increases, thus resulting in reduction of the filter passband magnitude. Fortunately, this reduction can be compensated by increasing pump power because these two laser sources individually play a role in generating filter passband. Furthermore, the bandwidth of each passband can be conveniently reconfigured through pulse modulation of pump wave^[10]. It is also of convenience to

be extended to provide multi-band bandpass filter response by adding more pump waves. However, the performance of our filter configuration drastically depends on the laser sources provided, including carrier and pumps. The major challenge is to mitigate the fluctuation of filter center frequency caused by wavelength shift of the laser source. An alternative solution based on modulation techniques is able to overcome this limitation due to the pump wave is generated by modulating optical carriers^[11].

In summary, we have proposed and experimentally demonstrated a dual-band bandpass MPF based on stimulated Brillouin scattering. Two passbands are generated respectively by mapping the gain spectra induced by two separated TLSs, and both passbands have the capability of independently tuning over a range from 1 GHz to 19 GHz. High resolution with 3 dB bandwidth less than 30 MHz and large out-of-band rejection about 40 dB under 25 mW optical pump power can be achieved.

References

- [1] G. Macchiarella and S. Tamiazzo, *IEEE Trans. Microw. Theory Tech.* **53**, 3265 (2005).
- [2] G. Chaudhary, Y. Jeong and J. Lim, *IEEE Trans. Microw. Theory Tech.* **61**, 107 (2013).
- [3] J. P. Yao, *J. Lightw. Technol.* **27**, 314 (2009).
- [4] J. Capmany, J. Mora, I. Gasulla, J. Sancho, J. Lloret and S. Sales, *J. Lightw. Technol.* **31**, 571 (2013).
- [5] L. Gao, J. Zhang, X. Chen and J. Yao, *IEEE Trans. Microw. Theory Tech.* **62**, 380 (2014).
- [6] R. Tao, X. Feng, Y. Cao, Z. Li and B. Guan, *IEEE Photon. Technol. Lett.* **24**, 1097 (2012).
- [7] W. Zhang and R. A. Minasian, *IEEE Photon. Technol. Lett.* **24**, 1182 (2012).
- [8] J. Guo, K. Wu, Y. C. Xiao and W. Dong, *Journal of Optoelectronics-Laser* **25**, 1274 (2014). (in Chinese)
- [9] Q. Wang, Y. Y. Shen, E. M. Xu and P. L. Li, *Journal of Optoelectronics-Laser* **26**, 1248 (2015). (in Chinese)
- [10] T. Tanemura, Y. Takushima and K. Kikuchi, *Opt. Lett.* **27**, 1552 (2002).
- [11] W. Zhang and R. A. Minasian, *IEEE Photon. Technol. Lett.* **23**, 1775 (2011).